CEBAF PROPOSAL COVER SHEET

This Proposal must be mailed to:

CEBAF
Scientific Director's Office
12000 Jefferson Avenue
Newport News, VA 23606

and received on or before 1 October 1991.

A. TITLE:

Helicity Structure of Pion Photoproduction

B. CONTACT PERSON:

D. I. Sober

ADDRESS, PHONE, AND ELECTRONIC MAIL ADDRESS:

Physics Department, Catholic University, 620 Michigan Ave.
Washington, DC 20064
Tel.: (202) 319-5856
Bitnet: Sober@CUA

C. IS THIS PROPOSAL BASED ON A PREVIOUSLY SUBMITTED PROPOSAL OR LETTI OF INTENT?

[ ] YES [X] NO

IF YES, TITLE OF PREVIOUSLY SUBMITTED PROPOSAL OR LETTER OF INTENT

****

(CEBAF USE ONLY)

Receipt Date 1 OCT 91

Log Number Assigned PR 91-015

By [redacted]

Proposal to CEBAF PAC 5 October 1991

Helicity Structure of Pion Photoproduction

Hall Crannell, J. T. O'Brien, D. I. Sober (spokesman)
Catholic University of America, Washington, DC 20064

R. A. Arndt, J. R. Ficenec, D. A. Jenkins, L. D. Roper and R. L. Workman
Virginia Polytechnic Institute and State University Blacksburg, VA 24061

D. G. Crabb, J. S. McCarthy, R. M. Sealock and S. T. Thornton
University of Virginia, Charlottesville, VA 22901

B. A. Mecking and V. Burkert
CEBAF, Newport News, VA 23606

E. Hayward, D. R. Tilley, H. R. Weller and R. Chasteler
Duke University, Durham, NC 27706

W. J. Briscoe, W. R. Dodge and L. C. Maximon
George Washington University, Washington, DC 20052

B. G. Ritchie
Arizona State University, Tempe, AZ 85287

ABSTRACT

We propose to measure the helicity-1/2 and helicity-3/2 contributions to the differential cross section for the processes $\gamma p \rightarrow \pi^0 p$ and $\gamma p \rightarrow \pi^+ n$ at photon energies between 0.3 and 2.3 GeV. The experiment will use tagged photons produced by longitudinally polarized electrons, and a longitudinally polarized proton target in the CLAS detector.

The goals of the experiment are:
(1) to test the hitherto untested predictions of the helicity asymmetry by partial wave analyses.
(2) to evaluate accurately the single-pion photoproduction contribution to the Drell-Hearn-Gerasimov (DHG) sum rule.
(3) to use the helicity asymmetry as a new diagnostic tool in searching for evidence of poorly determined baryon resonances.
(4) to perform a preliminary evaluation of the contributions of other significant processes (particularly $\gamma p \rightarrow \pi^+ \pi^- p$) to the DHG sum rule

1. INTRODUCTION

Over the years the study of pion photoproduction has provided important information about the structure of the nucleon, despite the absence of high-quality polarization data. The prospect of accurate measurements of spin parameters in photoproduction using highly polarized beams and targets opens up a new era of investigations aimed at probing the spin structure of the nucleon. One of the most intriguing possibilities provided by such experiments is an experimental test of the Drell-Hearn-Gerasimov sum rule.

The Drell-Hearn-Gerasimov (DHG) sum rule[1,2,3] is given by

$$\int_{thr}^{\infty} (\sigma_{1/2} - \sigma_{3/2})/k \; dk = -2\pi^2\alpha\kappa_p^2/m_p^2 \qquad (1)$$

$$= -5.26\times10^{-7}\,\mathrm{MeV}^{-2} = -204.8\ \mu\mathrm{b}$$

where $\sigma_{1/2}$ and $\sigma_{3/2}$ are the total cross sections for hadron photoproduction on protons in the helicity 1/2 and 3/2 states, k is the laboratory photon energy, κ_p is the proton's anomalous magnetic moment, and m_p the proton mass. The lower limit of integration is the threshold for pion photoproduction, ≈150 MeV. The sum rule follows from very general assumptions: the dispersion relation for forward Compton scattering and the low-energy theorem for Compton scattering, together with the prediction of Regge pole models that $\sigma_{1/2}-\sigma_{3/2} \to 0$ as $k \to \infty$.

The DHG sum rule has become of particular interest in combination with measurements of the comparable integral $\Gamma_p = \int_0^1 g_1\,(x,Q^2)dx$ in deep inelastic leptoproduction by the EMC collaboration. Results of the EMC experiment[4] give values of $\Gamma_p = 0.130\pm.015\pm.018$ at $Q^2 \approx 4.8$ GeV^2 and $0.114\pm.021\pm.019$ at $Q^2 \approx 17.2$ GeV^2. Anselmino *et al.*[5] define the quantity

$$I(Q^2) = 2\ m_p^2/Q^2\ \Gamma_p$$

whose EMC values are ≈ .061 and .011 at 4.8 and 17.2 GeV^2 respectively. The DHG sum rule requires the low-Q^2 limit of this quantity to be

$$I(0) = -\tfrac{1}{4}\kappa_p^2 = -0.804.$$

Thus $I(Q^2)$ must change slope and magnitude rapidly in the low-Q^2 region to reach the $Q^2 = 0$ limit. Such behavior has been attributed to "higher-twist" terms which may explain anomalies in the interpretation of the spin of the proton from the EMC data.[5]

A direct experimental test of the DHG sum rule would require a measurement of the separate helicity contributions to the total photoproduction cross section, using circularly polarized tagged

photons incident on a longitudinally polarized hydrogen target. No such measurement has yet been undertaken.

There have been several evaluations of the contribution of single-pion photoproduction to the sum rule, using existing partial-wave analyses of photoproduction data up to about 1.2 GeV, which found that the sum rule was at least approximately satisfied by this single process. The published 1973 analysis of Karliner,[6] which evaluated the isospin contributions separately, found contributions I_{VV} = 219 μb, $I_{SS} \approx 0$ to 3 μb and I_{VS} = 39 μb, leading to a value for the proton of about 260 μb, or somewhat greater than the DHG sum rule value. A more recent analysis,[7] extending to 1.8 GeV, has given similar results.

It is important to realize that there is **no theoretical reason** for the sum rule to be exhausted by single-pion production, or by the energy region below 1.2 GeV. Because of the 1/k weighting of the cross section difference in (1), and because the photoproduction cross section (Figure 1) is largest near the $\Delta(1232)$ peak which is produced primarily in the helicity-3/2 state, it is to be expected that the largest contributions to the sum rule will be from the energy region below 500 MeV. However, as shown in Figure 2(a), any saturation of the sum rule at energies near 1.2 GeV would imply a very large cancellation between the helicity contributions at higher energies. As shown in Figure 2(b), even a modest (5% to 10%) helicity asymmetry above 1.2 GeV or in the non-single-pion processes would have substantial effects on the convergence of the sum rule integral.

In their original paper, Drell and Hearn[3] stated "It will be of great interest if experiment can verify directly the validity of Eq. (1) by proving that the difference $\sigma_P(\nu)-\sigma_A(\nu)$ either drops smoothly to zero or has big contributions of different signs and compensating magnitudes before settling down to zero as predicted by Regge pole analyses." This statement remains true. We here propose the first part of a systematic program to investigate the convergence of the DHG sum rule, with particular emphasis on the contribution of single-pion photoproduction. The reason for this approach is outlined in the following section.

2. EXPERIMENTAL CONSIDERATIONS FOR A SUM RULE TEST

2.1 Variables and observables

In the γp system, there are four possible values of initial-state helicity, λ_i=-3/2, -1/2, +1/2 and +3/2, as indicated in Figure 3. Parity conservation implies that the cross section, summed over final-state polarizations, depends only on the **absolute value** of the helicity, so there are two contributions to the differential cross section, which we denote by $d\sigma_{1/2}$ and $d\sigma_{3/2}$. (Henceforth "$d\sigma$"

will be taken to mean "$d\sigma/d\Omega$".) These contributions can be determined experimentally from measurements with circularly polarized photons incident on a longitudinally polarized proton target.

If the beam's circular polarization is denoted by P_{circ} and the proton target polarization by P_{targ}, we find that the fraction of the initial flux with helicity $\pm 1/2$ and $\pm 3/2$ is given by $\frac{1}{2}(1+P_{circ}P_{targ})$ and $\frac{1}{2}(1-P_{circ}P_{targ})$ respectively. If we let $P = |P_{circ} \cdot P_{targ}|$, then the measured cross section depends only on the relative sign of the beam and target polarizations,

$$\begin{aligned} d\sigma^+ &= \tfrac{1}{2}\{(1+P)d\sigma_{1/2} + (1-P)d\sigma_{3/2}\} \quad (P_{circ}P_{targ} > 0) \\ d\sigma^- &= \tfrac{1}{2}\{(1-P)d\sigma_{1/2} + (1+P)d\sigma_{3/2}\} \quad (P_{circ}P_{targ} < 0)\ . \end{aligned} \tag{2}$$

In an experiment, $d\sigma^+$ and $d\sigma^-$ are measured alternately by reversing the direction of polarization of the electron beam or of the target. Inverting Eq. (2) gives an expression for the difference $\Delta(d\sigma) \equiv d\sigma_{1/2} - d\sigma_{3/2}$ in terms of the cross sections observed in the two states of polarization:

$$\Delta(d\sigma) \equiv d\sigma_{1/2} - d\sigma_{3/2} = (1/P)\ (d\sigma^+ - d\sigma^-). \tag{3}$$

2.2 Problems in evaluating the sum rule

The difference of **total** cross sections which appears in the integrand of Eq. (1),

$$\Delta\sigma \equiv \sigma_{1/2} - \sigma_{3/2}\ , \tag{4}$$

is the integral of (3) over all angles, summed over all photoproduction processes. The experimental evaluation of $\Delta\sigma$, however, is far from straightforward, for two principal reasons:

(1) A direct measurement of a total cross section always entails some extrapolation to correct for detection efficiencies and missing solid angle. For some processes, however, the helicity-1/2 and helicity-3/2 cross sections may have very different angular distributions (Figure 4). This implies that a detailed and well-understood parameterization of each individual process is necessary in order to correct the total cross section for missing acceptance, and that the sum rule can be tested experimentally only by summing the contributions of **individual final states.**

(2) In a polarized proton target, the polarized free protons are outnumbered by a large factor (4.7 for ammonia, 6.4 for butanol) by the bound nucleons in the other nuclei. If all the bound-nucleon events are accepted, this dilutes the observed asymmetry,

requiring vastly increased running time for the same statistical error, and also introduces the possibility of large systematic errors in the subtraction of nearly equal numbers. These problems are alleviated if the free-proton events are separable from most of the bound-nucleon background by missing-mass or other kinematic cuts. This is possible when the reaction is one in which either all or all but one of the final-state particles are detectable with good energy and angular resolution.

For these reasons, the obvious place to begin an investigation of the DHG sum rule is with the two channels of single-pion photoproduction, $\gamma p \rightarrow \pi^0 p$ and $\gamma p \rightarrow \pi^+ n$. Each reaction is a two-body process with a detectable charged particle in the final state. These processes comprise nearly all of the total cross section up to 500 MeV, and, as described above, are expected to provide the major contribution to the sum rule. Furthermore, single-pion photoproduction can be described accurately in terms of partial wave analyses (PWA) which can be used in making the necessary acceptance corrections. These are discussed in the following section.

2.3 Partial wave analyses

Single-pion photoproduction can be parameterized in terms of helicity amplitudes based on a resonance description of the πN system,[8,9] and a number of independent partial wave analyses have been carried out over the past 20 years, using experimental data for the differential cross section and for transverse polarization parameters such as target asymmetry T, polarized photon asymmetry Σ, and recoil nucleon polarization P_N. There are ongoing programs of such analyses over the energy region from threshold to 1 GeV or higher at Glasgow,[10,11] Tokyo,[12] Nagoya,[13,14] and Virginia Tech (VPI).[15] Although the experimental data base is far from complete, the most recent analyses have considerable predictive power. For example, a recent measurement[16] of polarized target asymmetry in the inverse photoproduction reaction $\pi^- p \rightarrow \gamma n$ is in excellent agreement with the predictions of the VPI partial wave analysis, although the latter does not include the new data.

Each of these analyses makes specific predictions for the individual helicity contributions $d\sigma_{1/2}$ and $d\sigma_{3/2}$, or equivalently for the unpolarized differential cross section

$$d\sigma = \tfrac{1}{2}(d\sigma_{1/2} + d\sigma_{3/2}) \qquad (5)$$

and the helicity asymmetry parameter traditionally[9] called E (which we will always denote $E(\theta)$ to keep it from being confused with energy):

$$E(\theta) \equiv (d\sigma_{1/2}(\theta) - d\sigma_{3/2}(\theta)) / (d\sigma_{1/2}(\theta) + d\sigma_{3/2}(\theta)) \quad (6)$$

There are no measurements of $E(\theta)$ to test these predictions directly. Although the various partial wave analyses agree with each other near 300 MeV, in the region of the $\Delta(1232)$ resonance, there is substantial disagreement at all energies from 400 MeV upwards, as is shown in Figure 5. (The "data points" in Figure 5 illustrate the uncertainty expected from the proposed experiment, in 25-MeV bins of photon energy. There are as yet no experimental data.) A direct measurement of $E(\theta)$ would provide severe constraints on these analyses.

Most important from the point of view of the DHG sum rule is the fact that the partial wave analyses, suitably adjusted as needed to agree with the new $E(\theta)$ data, provide a framework for extrapolation to very forward and very backward angles. As can be seen in Figure 4, the π^+n cross section contains a substantial forward peak at most energies. This peak, however, is primarily due to Born terms and is fitted consistently by the various partial wave analyses. Furthermore, as the value of $E(\theta)$ is required by angular momentum conservation to be unity at 0° and 180°, the extreme forward and backward cross sections have little influence on the uncertainty in $\Delta\sigma$.

A direct measurement of $E(\theta)$ in fine steps of photon energy may also have important applications in the study of resonances in the πN system. Figure 6 shows the prediction of the VPI analysis for the energy dependence of $E(\theta)$ at two fixed center-of-mass angles. The rapid variations occur in the vicinity of various known resonances. Since $E(\theta)$ is directly related to the angular momentum quantum numbers of a resonant state, it is expected to be very sensitive to even relatively weak resonances. Figure 7 shows the consequences of omitting and including the weakly photo-excited $P_{11}(1440)$ "Roper" resonance from the VPI partial wave analysis. (The "data points" illustrate the uncertainty expected from the proposed experiment in 25-MeV bins of energy and angle bins of width 0.1 in $\cos\theta$.) It is evident that there is interest in measuring the polarization asymmetry in pion photoproduction quite apart from its contribution to the sum rule.

2.4 Converging on the sum rule

The primary goal of the proposed experiment is to evaluate the single-pion contribution to the DHG sum rule up to 2 GeV. It is not expected that any single experiment will produce a definitive value for the entire sum. The principal constituents of a concerted attack on the sum rule might be measurements of:

(a) single-pion photoproduction from .3 to 2 GeV

(b) multi-pion and other processes below 2 GeV

(c) all final states in the energy region 2 to 4 GeV

and possibly (**not** at CEBAF)

(d) single pion photoproduction from threshold to 300 MeV.

The present experiment is optimized for item (a), but will also provide a major part of item (b). A measurement of single-pion photoproduction with polarized photons and protons in the CLAS will be triggered not only on the single-pion events but also on all other processes with a charged particle in the final state. The most important of these processes is $\gamma p \rightarrow \pi^+\pi^- p$, which contributes about half of the non-single-pion total cross section up to 1.5 GeV. With only charged particles in the final state, this process will have a high efficiency for the detection of two or more particles, and can be subjected to missing-mass cuts. While the structure of this process is more complicated than that of $\gamma p \rightarrow \pi N$, it consists primarily of a discrete set of fairly well-understood contributions ($\gamma p \rightarrow \rho^0 p$, $\omega^0 p$, $\pi^+\Delta^0$, $\pi^-\Delta^{++}$) which should allow for correction of the acceptance in each helicity state with reasonable accuracy.

It should be noted that the helicity asymmetry for the photoproduction of a baryon resonance is independent of its decay channel. If the branching ratio of a resonance is known, then the photoproduction asymmetry measured by detection of a particular final state ($\pi^+ n$, $\pi^0 p$ or $\pi^+\pi^- p$) can also be applied to the other decay channels. In this way, it may be possible to place reasonably restrictive limits on the sum rule integral without explicitly measuring all non-negligible final states.

3. EXPERIMENTAL PROCEDURE

3.1 Kinematic region

We propose to measure the differential cross sections for single pion photoproduction with circularly polarized photons of energy from 0.3 to 2.3 GeV incident on a longitudinally polarized proton target in the CLAS. The lower limit of 300 MeV is the minimum photon energy for which the charged final-state particles can be detected effectively over a large part of the angular distribution (see below). This energy is approximately at the peak of the $\Delta(1232)$ resonance, and is an important calibration point because the helicity asymmetry is large and is predicted with unanimity by the partial wave analyses (Figure 5). The upper energy limit of 2.3 GeV is higher than the maximum energy of the partial wave analyses (1.8 GeV), and covers the entire region over which single pion production is an appreciable part

of the total cross section.

3.2 Circularly polarized photon beam

A circularly polarized photon beam is produced by bremsstrahlung of longitudinally polarized electrons. The circular polarization[17] is given approximately by

$$P_{circ} = P_{el} \, (4x-x^2)/(4-4x+3x^2) \qquad (7)$$

where $x = k/E_0$ (E_0 = electron energy, k = photon energy) and P_{el} is the longitudinal polarization of the electron. A more precise calculation[17] requires angular integration over the collimation aperture. Some results are plotted in Figure 8. With electron polarizations of 80% (achievable for low-current sources), the photon circular polarization will be ≈80% at the bremsstrahlung endpoint and >40% at $k/E_0 = 0.5$.

It is not yet clear whether such a high-polarization source will be available. The high-current polarized electron source which is now under development for CEBAF is expected to have a polarization of only 50%. The run time required for this experiment has been calculated for an assumed beam polarization of 50%. Availability of a source with 80% polarization will reduce the run time request by a factor of 2.5 (!).

The Hall B tagging system will be used to produce tagged photons at a rate of 10^7 per second. The photons must be collimated to a diameter consistent with the size of the polarized proton target, so the rate of photons on target will be less than the tagging rate. The photon energy region $0.3 < k < 2.3$ GeV can be covered by running with three electron energies: 0.8, 1.6 and 2.4 GeV. Because of the decrease of circular polarization with photon energy, the low-energy data can be measured more effectively by using a fourth electron energy of 0.5 GeV. In the rate and run time calculations below, both options are considered.

3.3 Polarized proton target

The experiment requires a polarized proton target which can be inserted into the CLAS. The University of Virginia group is working on a high-field (≈5 T) polarized ammonia target for Hall C, and this system can be made compatible with CLAS requirements, as shown in Figure 9. The experiment could be performed with such a target. The main effect of the target field on the outgoing particles above 150 MeV/c is an azimuthal deflection which has almost no influence on the accuracy of momentum and angle reconstruction.[18]

Since the present experiment is not affected by radiation-damage considerations, a better solution would be the construction of a frozen-spin target with a low (≈0.1 T) holding field, which would have a much smaller effect on low-momentum outgoing particles. The holding field could be produced by much less massive magnet coils, which would leave more of the solid angle available for particle detection. Butanol is preferable to ammonia as a target material because the bound nucleons are unpolarized; the better radiation resistance of ammonia is not of concern in a photon experiment.

3.4 Particle detection and background suppression

The outgoing π^+ from $\gamma p \rightarrow \pi^+ n$ and the outgoing proton from $\gamma p \rightarrow \pi^0 p$ will be detected in the CLAS. Table 1 shows the range of center-of-mass angles which will be detected with reasonable solid angle coverage. Above k ≈ 1 GeV, the angular acceptance is nearly complete. Below ≈700 MeV, the proton acceptance for $\pi^0 p$ at forward pion angles is limited in part by energy loss in the target. As indicated in Table I, some of this forward region can be covered by detecting the $\pi^0 \rightarrow \gamma\gamma$ decay in the forward shower counters. A detailed signal-to-noise analysis of this detection mode has not yet been carried out.

In order to observe a significant experimental helicity asymmetry it is necessary to eliminate the contribution of the bound nucleons in the target. This can be done by missing-mass cuts, as illustrated in Figure 10. The background calculation includes both single-pion and multi-pion production from both protons and neutrons in the C and O nuclei of the butanol target. It is assumed that pions and protons can always be distinguished. With reasonable cuts, the bound nucleons contribute backgrounds of order 50% under the free-nucleon peak (Table 2). Subtractions, or at least tight cuts, can be made if the shape of the bound-nucleon missing mass peak is known. Short data runs with a carbon target of appropriate average density will be taken to determine this shape. Since the bound nucleons in butanol are unpolarized, no further correction for this background is necessary.

4. STATISTICAL AND SYSTEMATIC UNCERTAINTIES

4.1 Criteria for a sum rule test

We assume that the ultimate goal of the program is a measurement of the DHG sum rule (Eq. (1)) to an accuracy of 10%, or 20 μb. The experimental quantity in the integrand of Eq. (1) is the difference in total cross sections $\Delta\sigma \equiv \sigma_{1/2} - \sigma_{3/2}$, integrated from the difference in differential cross sections and summed over all

final states. We make the following assumptions:

(a) The cross section must be evaluated in bins of width ≈25 MeV, consistent with the variations in the resonant structure of the cross section.
(b) The **statistical** uncertainties in the energy bins for each process are uncorrelated, and add in quadrature.
(c) The **statistical** uncertainties in the individual processes are uncorrelated.
(d) The **systematic** uncertainties are uniform over relatively large energy regions, and may be considered to add linearly over the energy bins.
(e) The **systematic** uncertainties may add linearly for the individual final states.
(f) The DHG integral must ultimately be evaluated between threshold (≈150 MeV) and ≈4 GeV, and the uncertainty in any energy region must be consistent with an uncertainty of 20 μb in the total.

If the systematic uncertainty in $\Delta\sigma$ were constant over the interval of interest, assumption (d) implies that the uncertainty in the integral I could be written

$$\delta_{sys}I = \delta_{sys}(\Delta\sigma)\ \ln(k_{max}/k_{min}). \qquad (8)$$

Setting k_{min}=0.15 GeV and k_{max}=4.0 GeV, δI=20 μb would require a systematic uncertainty $\delta_{sys}(\Delta\sigma)$ < 6.1 μb over the whole region, assuming that the statistical uncertainty can be made small compared with the systematic uncertainty. (The fact that we are not measuring below 300 MeV or above 2.3 GeV does not allow us to "use up" their allocation of uncertainty.) According to assumption (e), $\delta_{sys}(\Delta\sigma)$ may be apportioned among the contributing processes according to their fraction of the total cross section, so $\delta_{sys}(\Delta\sigma)$ for each of π^+n and π^0p should be < 3 μb below 0.5 GeV, decreasing to about 0.5 μb at 2 GeV.

Except near the peak of the $\Delta(1232)$ resonance, this requirement on $\delta_{sys}(\Delta\sigma)$ is never less than ≈10% of $\Delta\sigma$. Many of the experimental systematics cancel out in taking the difference of helicity contributions, so the goal is not unreasonable. Over much of the energy region, the unpolarized cross section is well known from other experiments and partial wave analyses, so the present experiment need only provide a measurement of the helicity asymmetry $E(\theta)$, whose systematic uncertainty will be smaller than that on $\Delta(d\sigma)$. In the $\Delta(1232)$ region, as mentioned above, the helicity structure of photoproduction is already well understood, and this experiment is not expected to provide new data; the measurements near 300 MeV will be taken primarily as a calibration.

In accordance with assumptions (a) and (b) above, a constant

statistical uncertainty $\delta_{stat}(\Delta\sigma)$ in each energy bin of width Δk will give a statistical uncertainty in the sum rule

$$\delta_{stat}I = \delta_{stat}(\Delta\sigma)\ [\Delta k\cdot(1/k_{min} - 1/k_{max})]^{1/2} . \qquad (9)$$

Taking $\delta_{stat}(\Delta\sigma)$ <10 μb for each 25-MeV bin (or < 7 μb for each of π^+n and π^0p) would give a contribution $\delta_{stat}I$ < 4 μb, which is much smaller than the estimated contribution of systematic uncertainties. (For a given total number of events, the statistical uncertainty in the sum rule is not sensitive to the bin width.)

4.2 Systematic uncertainties

The goal of $\delta_{sys}(\Delta\sigma)$ < 6 μb everywhere sounds like a stringent condition when compared to the unpolarized total cross section, but is actually at least 10% of the cross section difference $\Delta\sigma \equiv \sigma_{1/2}-\sigma_{3/2}$ everywhere except near the peak of the $\Delta(1232)$. We estimate the principal systematic uncertainties as follows:

Factors which largely cancel in the asymmetry:	
photon flux	±2%
target thickness	±3%
azimuthal acceptance	±2%
Factors which directly affect the asymmetry:	
electron beam polarization	±5% of P_{elec}
target polarization	±3% of P_{targ}
extrapolation to unmeasured angles	±5%

The resulting systematic uncertainty in $\Delta\sigma$ is estimated at ±8%.

In each energy region it must be decided whether the unpolarized differential cross section is already known to better precision than the normalization factors other than polarizations. If so, the experiment will determine only the asymmetry $E(\theta)$ and use the prior measurements of $d\sigma$ to determine $\Delta(d\sigma)$.

4.3 Statistical uncertainties

The statistical uncertainty in the difference of cross sections is given by

$$\delta_{stat}(\Delta\sigma) = [2\sigma(1+B)/P]\ (n^+ + n^-)^{-1/2}$$

$$= 2\sigma/P\ \{(1+B)/(n^+_{free}+n^-_{free})\}^{1/2} \qquad (10)$$

where σ is the unpolarized cross section, B is the number of bound nucleons per free contributing to the measurement after

kinematic cuts, P is the product of photon and target polarizations, n^+ and n^- are the number of events per bin (including bound nucleon events after cuts) in the two relative polarization states, and n^+_{free} and n^-_{free} are the corresponding number of events from the free protons alone. The same expression also applies for the differential cross section in an angular bin, with $\Delta d\sigma$ and $d\sigma$ replacing $\Delta\sigma$ and σ.

The statistical uncertainty in the difference of total cross sections is the result of adding uncorrelated statistical uncertainties in the angular bins of differential cross section. This is approximately true even if the angular integration is performed by means of fitting the data to a parameterization. The variation in the angular distribution requires that data be binned in approximately 20 bins of $\cos\theta$. The requirement $\delta_{stat}(\Delta\sigma) = 10$ μb in each 25-MeV bin of photon energy corresponds to an uncertainty $\delta_{stat}(\Delta d\sigma) = 2.2$ μb/sr in each bin of $\cos\theta$, or about 1.5 μb/sr for each πN final state below $\approx$500 MeV, decreasing to about 0.7 μb/sr at 2 GeV. The angular binning has little effect on the sum rule test, but governs the statistical precision in the helicity asymmetry $E(\theta)$, which is given by

$$\begin{aligned} \delta_{stat}E(\theta) &\approx (1+B)/P\ (n^+ + n^-)^{-1/2} \\ &= 1/P\ \{(1+B)/(n^+_{free}+n^-_{free})\}^{1/2} \end{aligned} \qquad (11)$$

with all symbols defined as in Eq. (10).

Since the extrapolation to unmeasured forward and backward angles depends on the validity of the partial wave analysis fits, it is important that these be properly constrained by the data. Thus our final condition for significance is that the helicity asymmetry parameter be determined to better than $\delta_{stat}E(\theta) < 0.10$ at all measured energies and angles.

4.4 Count rates and run times

The counting rates are estimated using the following conservative assumptions:

10^7 tagged photons/sec in the specified energy range
target thickness: 2 g/cm^2 butanol
target diameter: 2 cm (photon beam collimated to 2 cm)
geometrical efficiency: 50% of 4π solid angle
electron polarization: 50%
target polarization: 70%
energy bin width: 25 MeV
angle bin width: $\Delta\cos\theta = 0.10$
bound/free nucleon contamination ratio after cuts:
0.7 to 2.5 (see Table 2)

In order to cover the energy range 0.3 - 2.3 GeV without using circular polarizations of less than 50% of the electron polarization, we would require 4 settings of the electron energy: 0.5, 0.8, 1.6 and 2.4 GeV. However, it appears that using a single electron energy of E_0 = 0.8 Gev to cover the region 0.30 < k < 0.76 GeV instead of requiring endpoint energies of both 0.5 and 0.8 GeV gives comparable statistical precision for the same run time, despite the very low circular polarization at the low-k end. However, a detailed study of systematic uncertainties may eventually favor running at both 0.5 GeV and 0.8 GeV.

At each energy setting, two runs are required: a long run with the polarized butanol target, and a short run (about 15% of the run time) with a carbon dummy target. The carbon runs are required to determine the shape of the bound-nucleon contribution under the two-body missing-mass peaks, allowing tighter cuts to be applied. During each run, the sign of the electron beam polarization will be alternated frequently to minimize systematic errors.

The following run times are required to meet the stated goals of statistical accuracy:

Electron Energy (GeV)	k_{min} (GeV)	k_{max} (GeV)	Run time (hours)
0.80	0.28	0.47	120 + 20 = 140
1.60	0.65	1.52	120 + 20 = 140
2.40	1.40	2.28	120 + 20 = 140
(Beam polarization = 50%)			Total hours = 420

If a beam polarization of 80% is available instead of the assumed 50%, the run times could be reduced by a factor of 2.5 for the same statistical uncertainty. The shortness of the runs would then lead to some additional overhead, so the estimate becomes

(Beam polarization = 80%) Total hours = 220

Table 3 gives some resulting count rates, valid for either case. If the CLAS detector is triggered by all detected charged particles, the count rate at 2.4 GeV electron energy would be close to the limits of the system (≈6 kHz singles, reals ≈ accidentals ≈ 600 Hz), but this could be reduced substantially by imposing simple momentum cutoffs in the trigger electronics.

Some examples of the estimated statistical uncertainty in the cross section difference $\Delta(d\sigma)$ and in the helicity asymmetry $E(\theta)$ are given in Table 4 and Table 5 respectively. Fictitious "data points" showing the estimated total uncertainty (statistical and

8% systematic) in $E(\theta)$ are plotted in Figures 5 and 7.

The experiment is certainly sensitive to differences in the partial wave analyses, justifying the measurement quite apart from the DHG sum rule test.

With the requested run time allotment of 420 hours, the experiment can measure directly the single-pion contribution to the DHG sum rule up to 2.2 GeV, with an overall accuracy of better than 20 μb or 10%.

Because the CLAS trigger will include events from other charged-particle final states, this experiment will also provide data on the helicity asymmetry in other important final states. The analysis of these processes is considerably more complicated than that of the single-pion production data, and no detailed calculations have yet been undertaken. As mentioned above, we expect that the important $\pi^+\pi^-$p final state will be reasonably tractable. Analysis of this process will give a first measurement of the contribution to the DHG sum rule of approximately half of the non-single-pion cross section up to 2 GeV.

As mentioned in Section 2.4, a comprehensive test of the DHG sum rule will not be performed in a single experiment, but the measurement proposed here will be an essential contribution and an important first step.

REFERENCES

1. L. I. Lapidus and Chou Hangchao, Sov. Phys. JETP **14**, 1102 (1962).

2. S. B. Gerasimov, Sov. J. Nucl. Phys. **2**, 430 (1966).

3. S. D. Drell and A. C. Hearn, Phy. Rev. Lett. **16**, 908 (1966).

4. J. Ashman *et al.*, Nucl. Phys. **B328**, 1 (1989).

5. M. Anselmino, B. L. Ioffe and E. Leader, Sov. J. Nucl. Phys. **49**, 136 (1989).

6. I. Karliner, Phys. Rev. D **7**, 2717 (1973).

7. R. L. Workman and R. A. Arndt, "Saturation of the Drell-Hearn-Gerasimov Sum Rule Revisited," preprint, VPI&SU, Blacksburg, VA (1991).

7. R. L. Walker, Phys. Rev. **182**, 1729 (1969).

9. I. S. Barker, A. Donnachie and J. K. Storrow, Nucl. Phys. **B79**, 431 (1974); **B95**, 347 (1975).

10. F. A. Berends and A. Donnachie, Nucl. Phys. **B84**, 342 (1975); **B136**, 317 (1978).

11. R. L. Crawford *et al.*,*Proceedings of the IV International Conference on Baryon Resonances*, Toronto, 1980, p. 107.

12. I. Arai and H. Fujii, Nucl. Phys. **B194**, 251 (1982).

13. P. Feller *et al.*, Nucl. Phys. **B104**, 219 (1976).

14. R. Kajikawa *et al.*,*Proceedings of the IV International Conference on Baryon Resonances*, Toronto, 1980, p. 43.

15. R. A. Arndt, R. L. Workman, Z. Li and L. D. Roper, Phys. Rev. C **42**, 1853 (1990); Z. Li, R. A. Arndt, L. D. Roper and R. L. Workman, unpublished.

16. G. J. Kim *et al.*, Phys. Rev. D **43**, 687 (1991).

17. H. Olsen and L. C. Maximon, Phys. Rev. **114**, 887 (1959). Our Eq. (2) is derived from their Eq. (8.11).

18. V. Burkert *et al.*, CLAS Note 90-04, "Polarized Target Experiments Using the CEBAF Large Acceptance Spectrometer."

Table 1

Approximate limits on cos θ_{CM} accepted by the CLAS for single pion photoproduction.

Reaction:	$\gamma p \rightarrow \pi^+ n$	$\gamma p \rightarrow \pi^0 p$	
Particle:	π^+	proton	$\pi^0 \rightarrow \gamma\gamma$[1]
Photon energy	cos θ	cos θ	cos θ
300 MeV	-.80 to +.95	-.85 to +.20[2]	.70 to 1.00
500 MeV	-.88 to +.95	-.85 to +.70[2]	.60 to 1.00
700 MeV	-.90 to +.95	-.85 to +.80[2]	.45 to 1.00

Notes: [1] assuming 45° shower counter coverage
[2] including effects of proton range in target

Table 2

Ratio of bound-nucleon to free-nucleon events in the data sample after missing-mass cuts, estimated by Monte Carlo calculations.

	Bound:free event ratio			
k =	0.7 GeV	1.0 GeV	1.5 GeV	2.0 GeV
$\pi^+ n$	0.55	0.60	0.86	1.11
$\pi^0 p$	0.70	1.48	2.12	2.51

Table 3

Run times and rates assuming 10^7 tagged photons per second in the photon energy range $k_{min} < k < k_{max}$, collimated to a target diameter of 2 cm. The count rate assumes a butanol target of thickness 2 g/cm^2, and an average geometrical efficiency of 0.5. Approximately 15% of the run time is for a dummy carbon target (e.g. 120 hr + 20 hr = 140 hr).

E_0 (GeV)	k_{min} (GeV)	k_{max} (GeV)	Run time (hr)	Tagged γ/sec on target[1] ($\times 10^6$)	Total CLAS rate[2] (Hz)	Tagged real rate (Hz)	Accid. rate[2] (Hz)
0.80	0.28	0.76	140	2.70	670	500	20
1.60	0.70	1.52	140	5.69	2300	720	160
2.40	1.40	2.28	140	7.33	6400	650	570

Notes: [1] After collimation to 2 cm target diameter.

[2] Total rate and accidental rate assumes all events above threshold (k=150 MeV) contribute with equal efficiency (certainly an overestimate). Simple on-line momentum cuts will reduce these rates substantially for the higher-energy runs.

Table 4.

Statistical uncertainty in $\Delta(d\sigma) = d\sigma_{1/2}/d\Omega - d\sigma_{3/2}/d\Omega$ (in μb/sr), for 25 MeV bins in photon energy and angle bins of width $\Delta\cos\theta$=0.1, assuming the run times given in Table 3 (140 hours total for each energy) and an electron beam polarization P_e = 0.50. (If P_e = 0.8, the beam time will be reduced accordingly.)

		$\gamma p \rightarrow \pi^+ n$			$\gamma p \rightarrow \pi^0 p$		
		$\delta_{stat}\Delta(d\sigma)$ (μb/sr) for $\cos\theta_{CM}$=			$\delta_{stat}\Delta(d\sigma)$ (μb/sr) for $\cos\theta_{CM}$=		
E_0 (GeV)	k (GeV)	-.75	0.0	.75	-.75	0.0	.75
0.8	0.3	0.794	0.820	0.582	0.821	0.984	0.774
0.8	0.5	0.260	0.357	0.431	0.227	0.324	0.284
0.8	0.7	0.269	0.378	0.442	0.184	0.257	0.170
1.6	0.7	0.300	0.423	0.493	0.207	0.289	0.190
1.6	1.0	0.221	0.174	0.367	0.251	0.201	0.235
1.6	1.5	0.105	0.117	0.212	0.151	0.160	0.226
2.4	1.5	0.082	0.093	0.167	0.119	0.128	0.178
2.4	1.8	0.058	0.106	0.173	0.099	0.085	0.087
2.4	2.2	0.062	0.112	0.186	0.104	0.089	0.094

Table 5.

Statistical uncertainty in helicity asymmetry $E(\theta)$, for 25 MeV bins in photon energy and angle bins of width $\Delta\cos\theta$=0.1, assuming the run times given in Table 3 (140 hours total for each energy) and an electron beam polarization P_e = 0.50. (If P_e = 0.8, the beam time will be reduced accordingly.)

		$\gamma p \rightarrow \pi^+ n$			$\gamma p \rightarrow \pi^0 p$		
		$\delta_{stat}E(\theta)$ for $\cos\theta_{CM}$=			$\delta_{stat}E(\theta)$ for $\cos\theta_{CM}$=		
E_0 (GeV)	k (GeV)	-.75	0.0	.75	-.75	0.0	.75
0.8	0.3	0.019	0.018	0.026	0.020	0.017	0.021
0.8	0.5	0.034	0.025	0.020	0.043	0.030	0.034
0.8	0.7	0.030	0.022	0.018	0.048	0.034	0.052
1.6	0.7	0.034	0.024	0.021	0.054	0.039	0.057
1.6	1.0	0.032	0.041	0.019	0.045	0.057	0.047
1.6	1.5	0.075	0.068	0.037	0.089	0.084	0.059
2.4	1.5	0.060	0.054	0.030	0.071	0.066	0.046
2.4	1.8	0.084	0.047	0.027	0.082	0.097	0.092
2.4	2.2	0.089	0.050	0.031	0.087	0.102	0.097

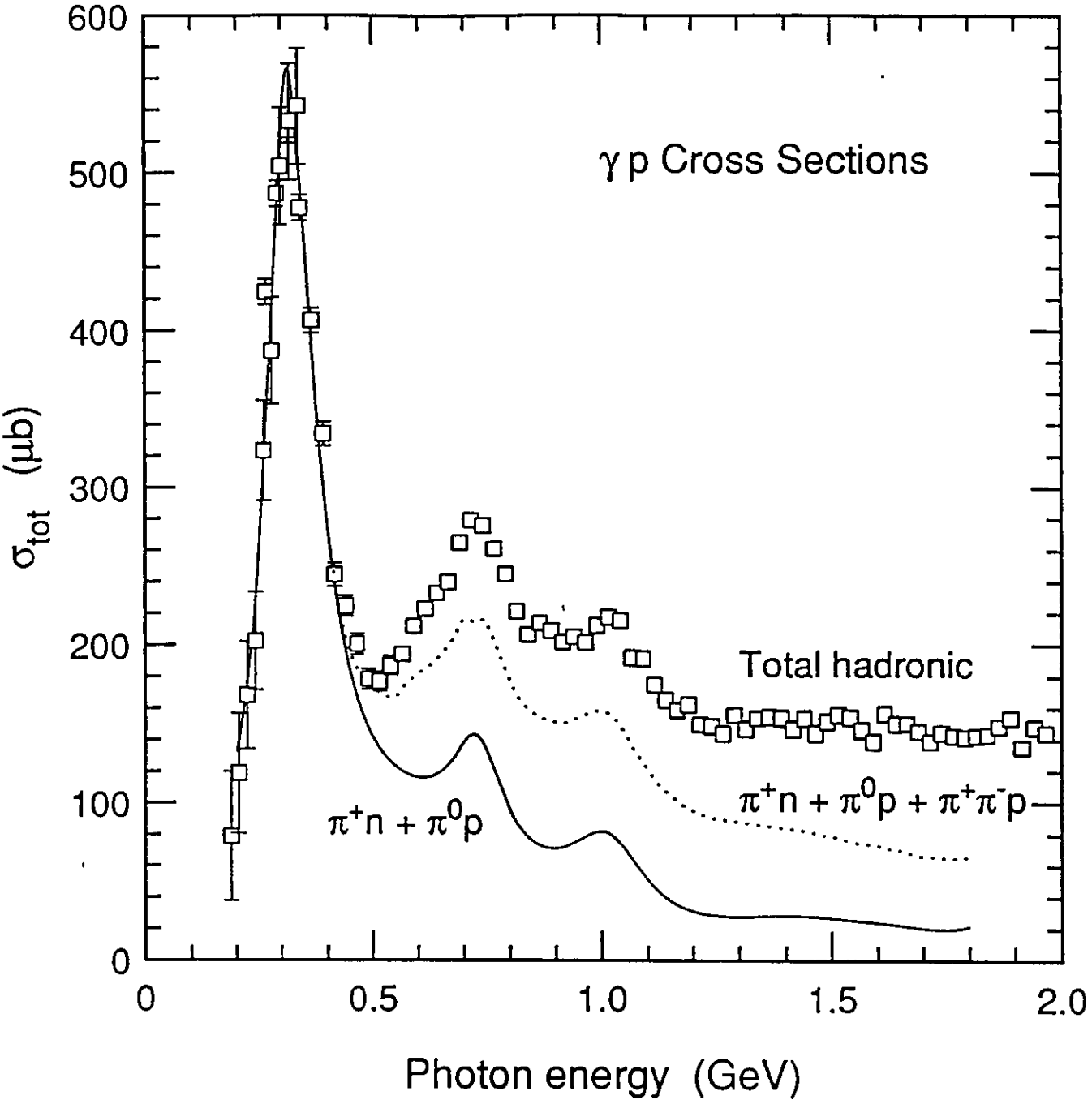

Figure 1. Single pion photoproduction (sum of $\gamma p \to \pi^+ n$ and $\gamma p \to \pi^0 p$, calculated from the VPI partial wave analysis), single pion photoproduction plus $\gamma p \to \pi^+ \pi^- p$, and the total cross section for $\gamma p \to$hadrons (data collected by A. Baldini, V. Flaminio, W.G. Moorhead and D.R.O. Morrison, *Total Cross-Sections for Reactions of High Energy Particles*, Landolt-Börnstein, New Series, Vol. 12b (1987).

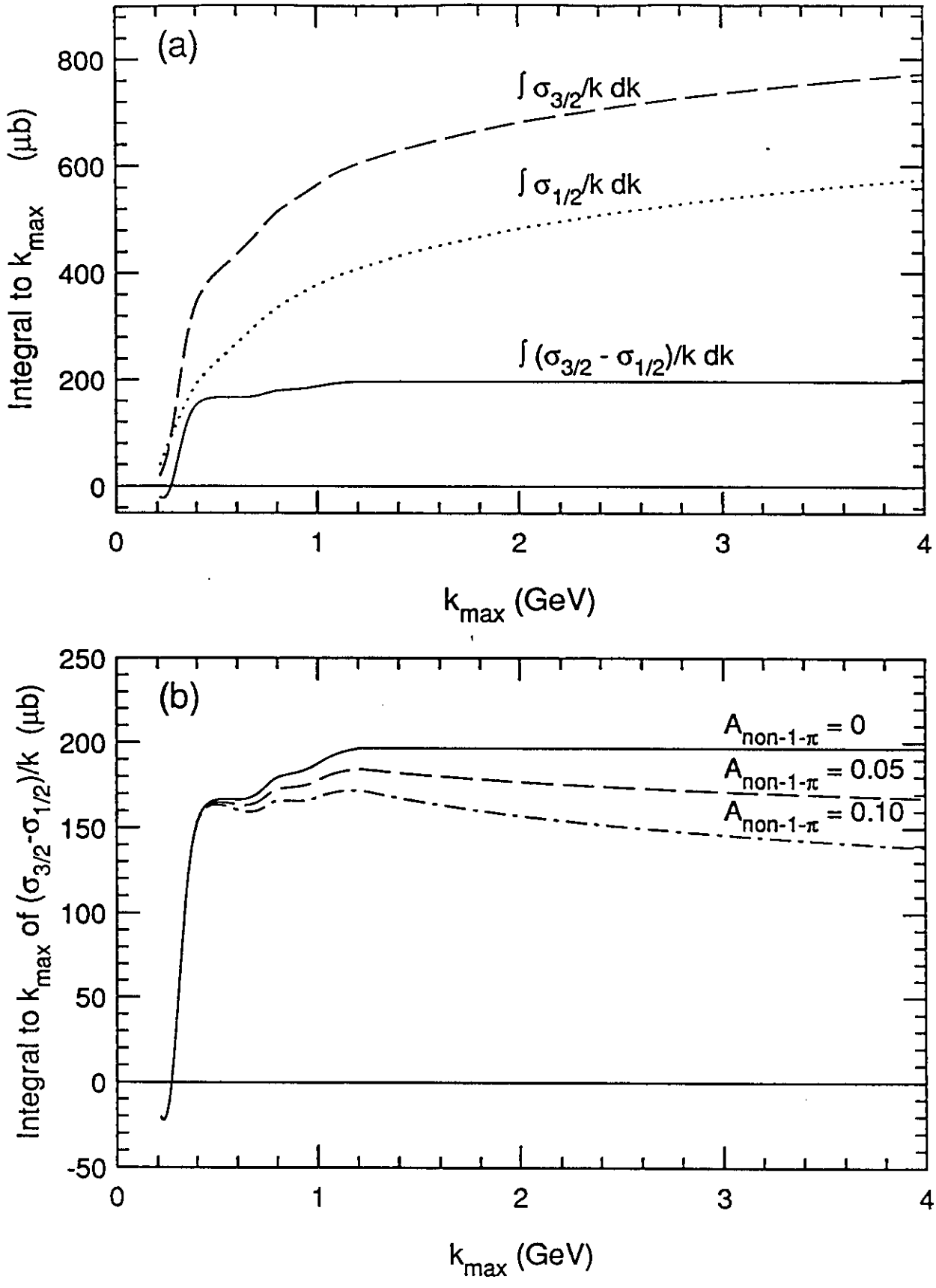

Figure 2. (a) Convergence of DHG integral as a function of the upper energy limit k_{max}, compared with the integrals of the separate helicity contributions, using Ref. 7 partial wave analysis for $\gamma p \rightarrow \pi N$, and assuming no helicity asymmetry in the remainder of the total cross section. (b) Convergence of DHG integral using 3 different assumptions for constant helicity asymmetry in the non-$\gamma p \rightarrow \pi N$ cross section.

Definition of helicity states:

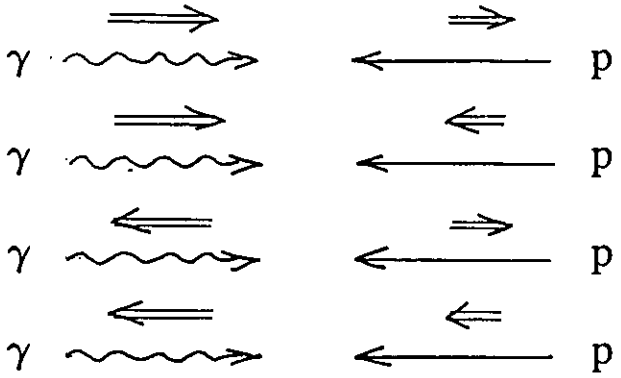

Measurement of helicity contributions:

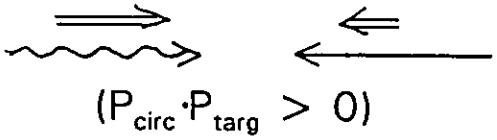

$(P_{circ} \cdot P_{targ} > 0)$

$$\sigma^{+} = \tfrac{1}{2}\{(1+P)\sigma_{1/2} + (1-P)\sigma_{3/2}\}$$

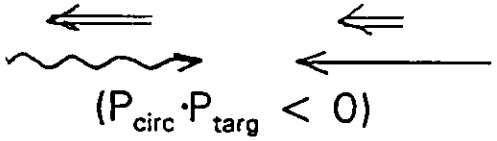

$(P_{circ} \cdot P_{targ} < 0)$

$$\sigma^{-} = \tfrac{1}{2}\{(1-P)\sigma_{1/2} + (1+P)\sigma_{3/2}\}$$

$$P \equiv |P_{circ} \cdot P_{targ}|$$

Figure 3. Definition of helicity states in the γp system, and the relation of the measured cross sections σ^{+} and σ^{-} to the helicity contributions and experimental polarizations.

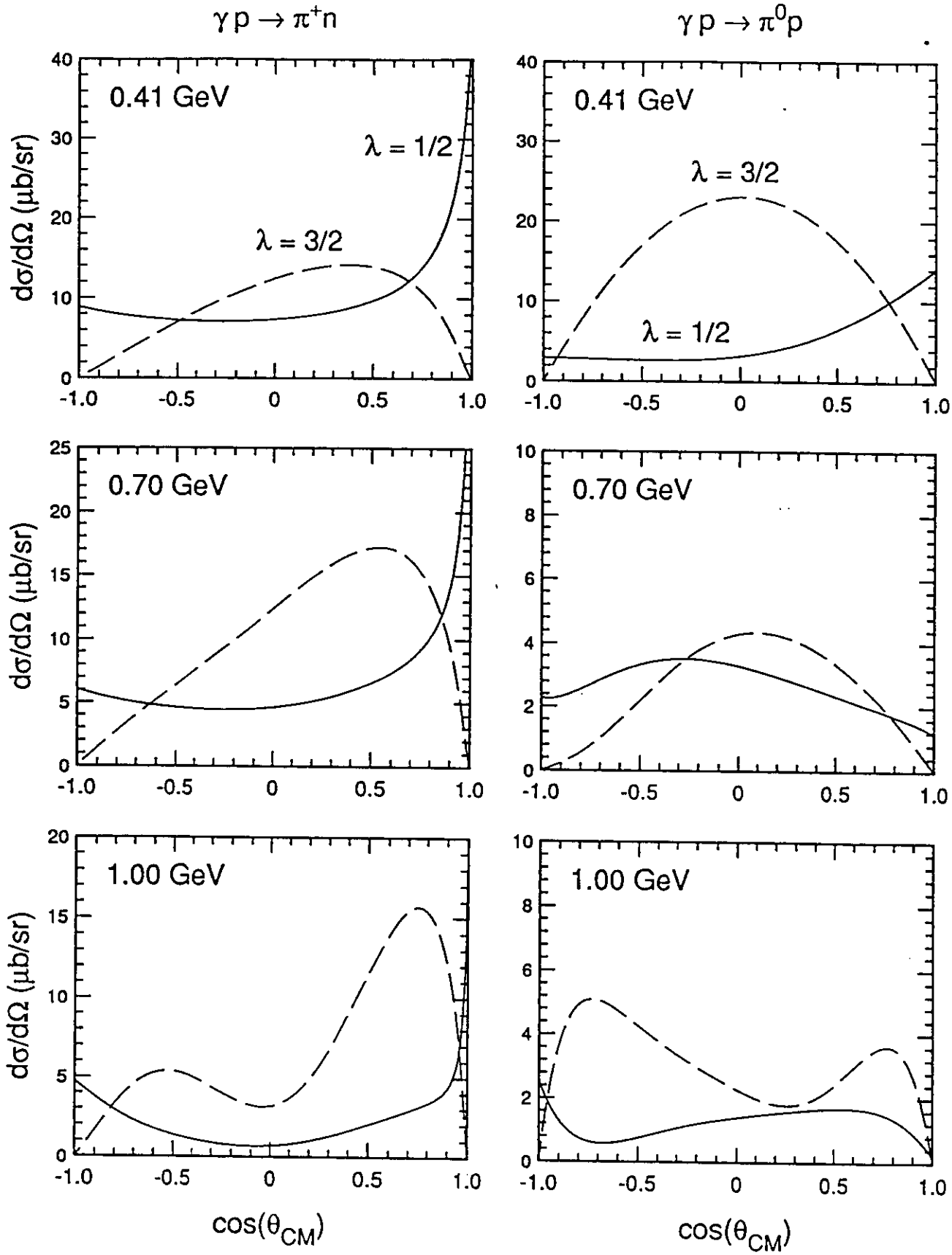

Figure 4. Predictions of the VPI partial wave analysis (Ref. 15) for the separate helicity contributions to the differential cross section, $d\sigma_{1/2}/d\Omega$ and $d\sigma_{3/2}/d\Omega$, for $\gamma p \rightarrow \pi^+ n$ (left column) and $\gamma p \rightarrow \pi^0 p$ (right column), at three photon energies.

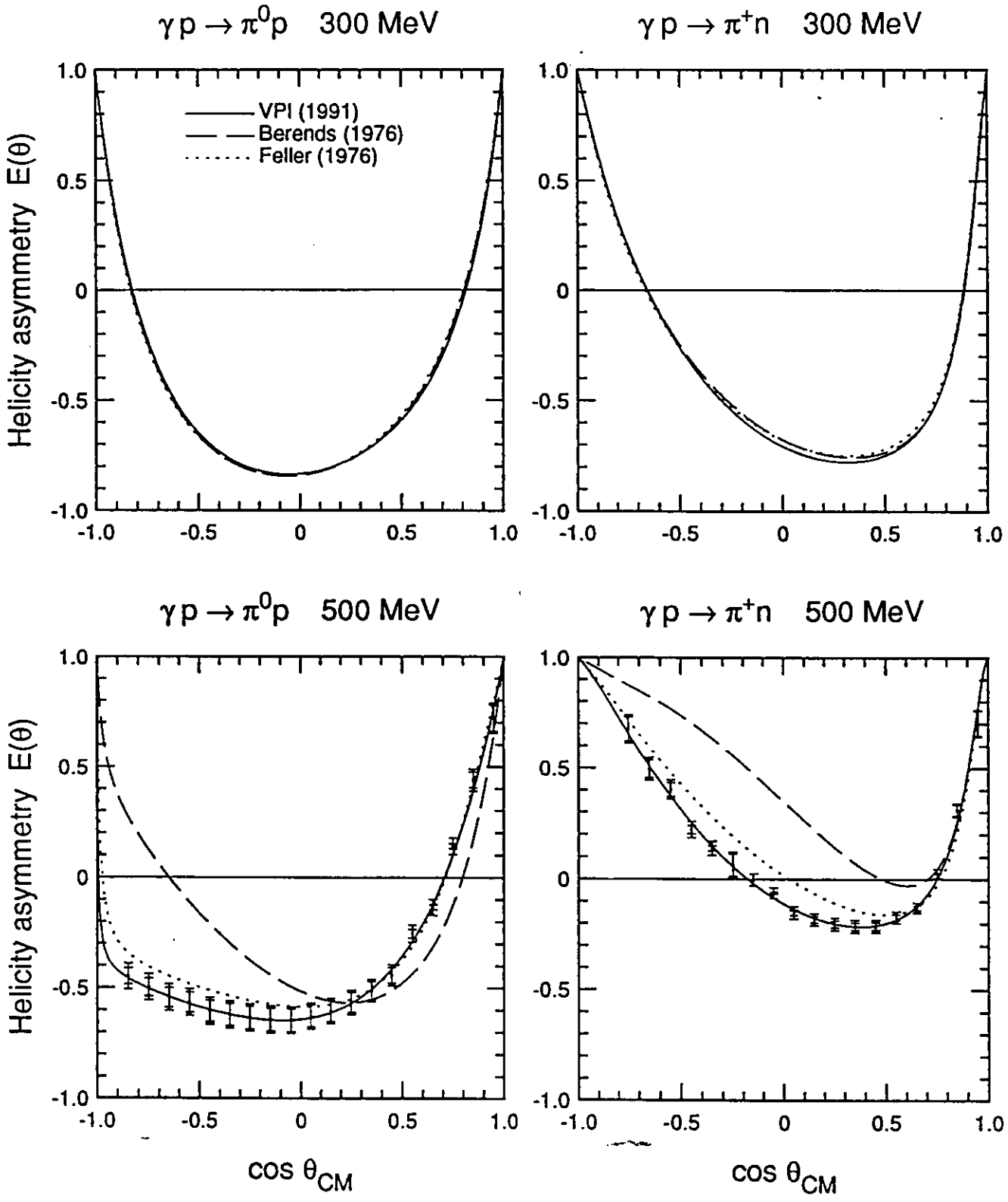

Figure 5. Helicity asymmetry $E(\theta)$ in $\gamma p \to \pi^+ n$ (left column) and $\gamma p \to \pi^0 p$ (right column), predicted by several different partial wave analyses: solid = VPI (Ref. 15), dashed = Glasgow (Ref. 10), dotted = Nagoya (Ref. 13). The "data points" show the estimated uncertainties resulting from this experiment: inner error bars = systematic, outer error bars = systematic and statistical (in a 25 MeV energy bin).

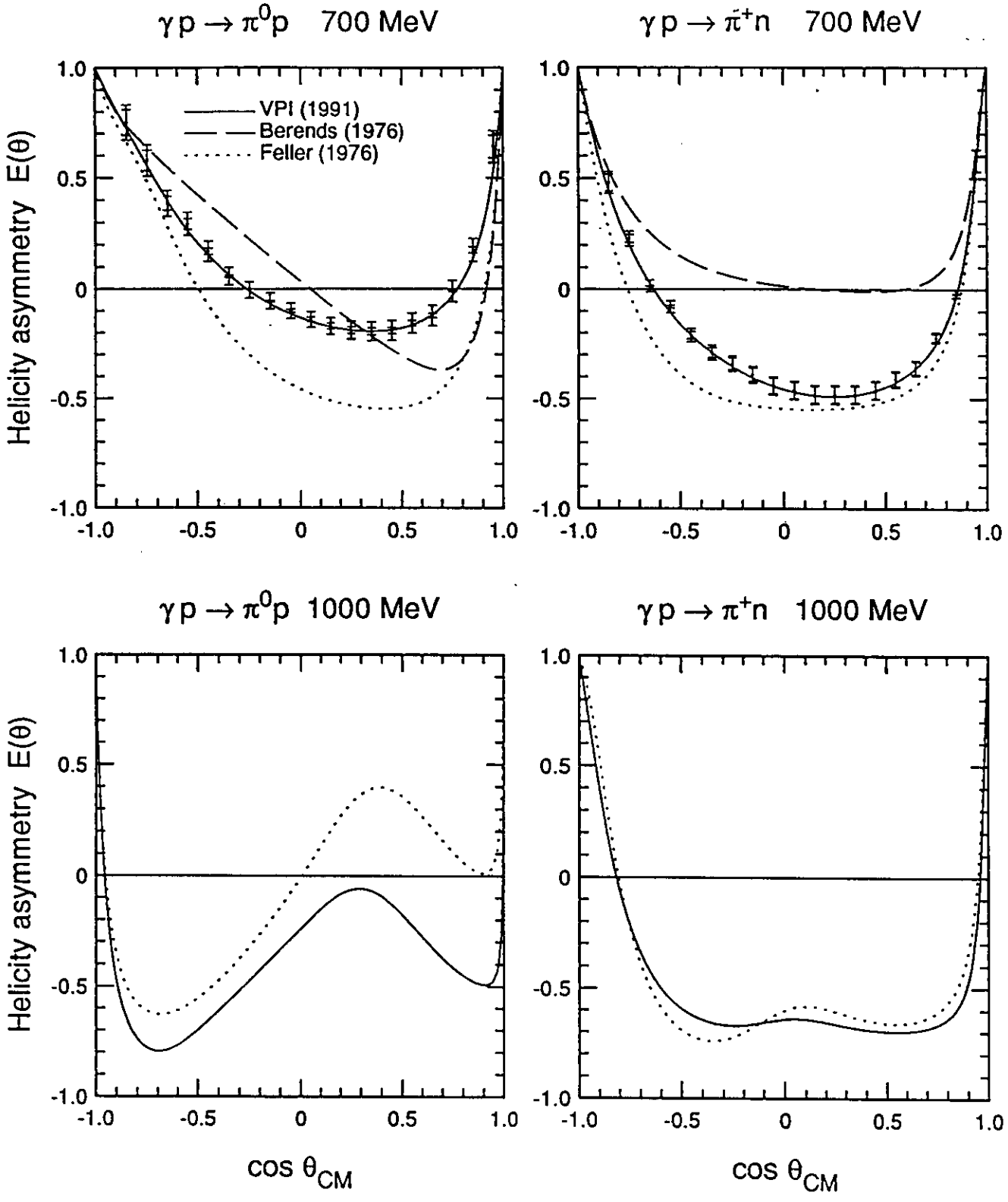

Figure 5 -- continued

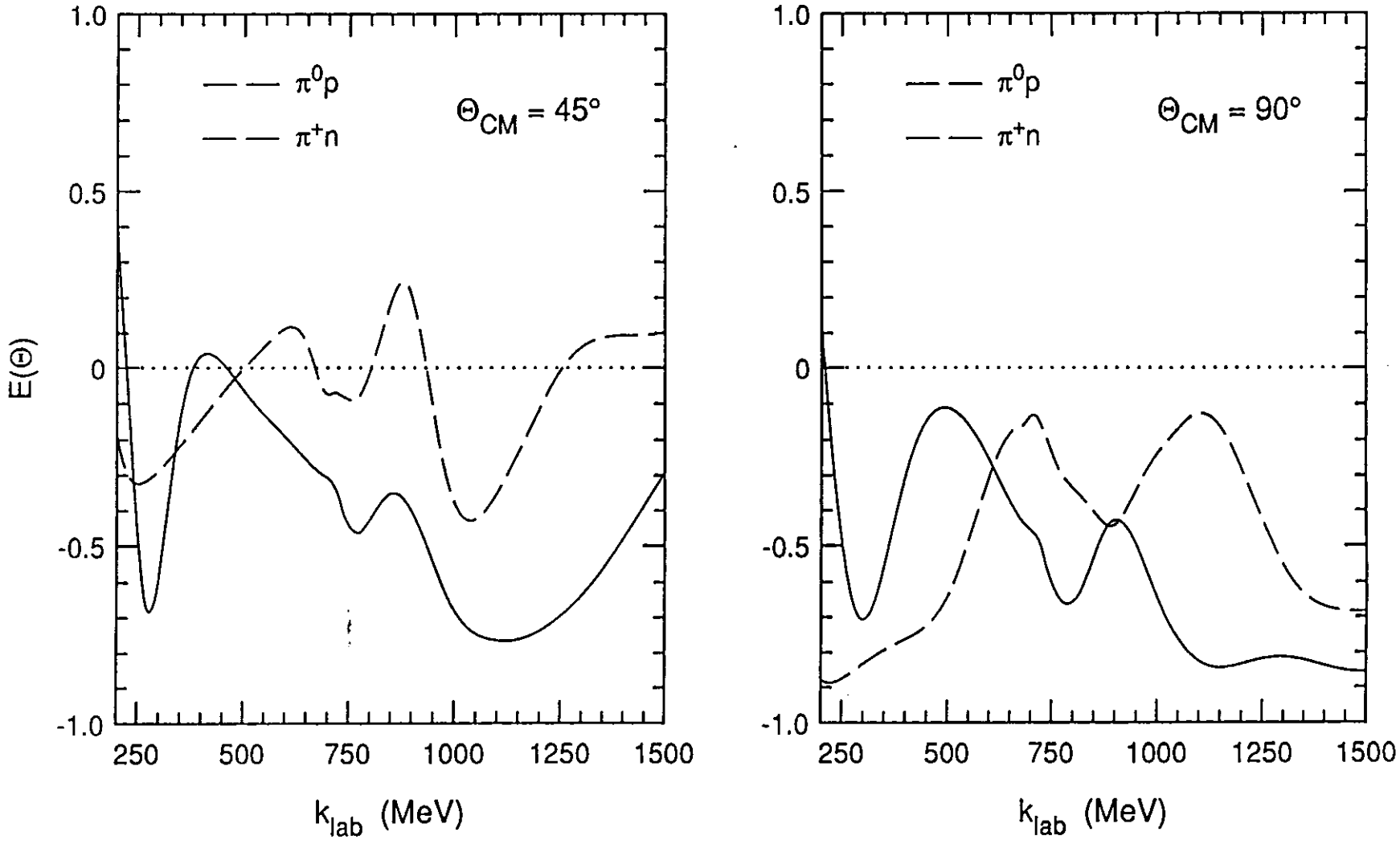

Figure 6. Energy dependence of the helicity asymmetry $E(\theta)$ at fixed center-of-mass angles, as predicted by the VPI partial wave analysis.[15]

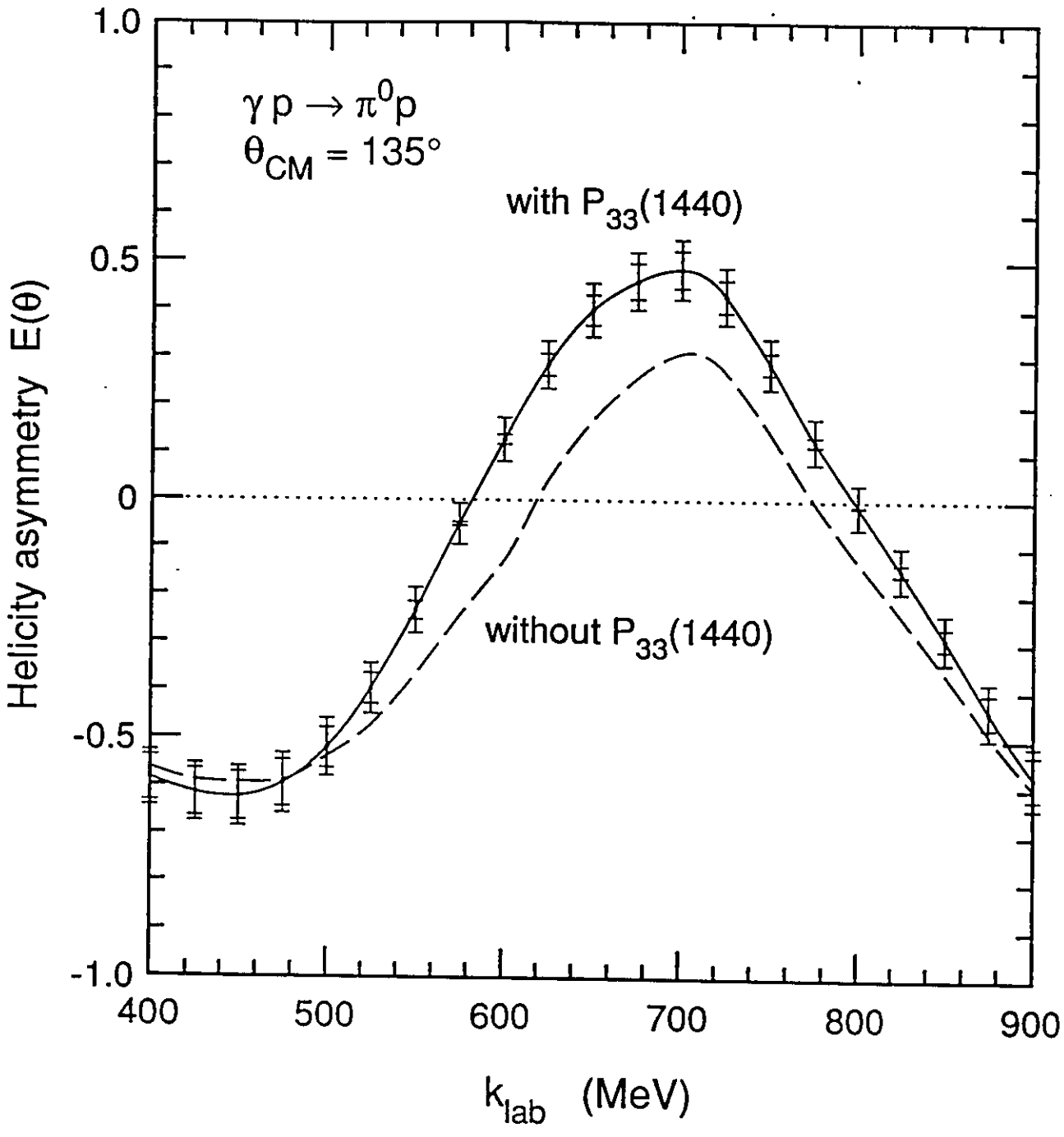

Figure 7. Energy dependence of $E(\theta)$ at $\theta_{CM} = 135°$ calculated by the VPI partial wave analysis[15] with and without the $P_{11}(1440)$ resonant amplitudes included. The "data points" show the estimated uncertainties resulting from this experiment: inner error bars = systematic, outer error bars = systematic and statistical (in an angle bin of 0.10 in $\cos\theta$).

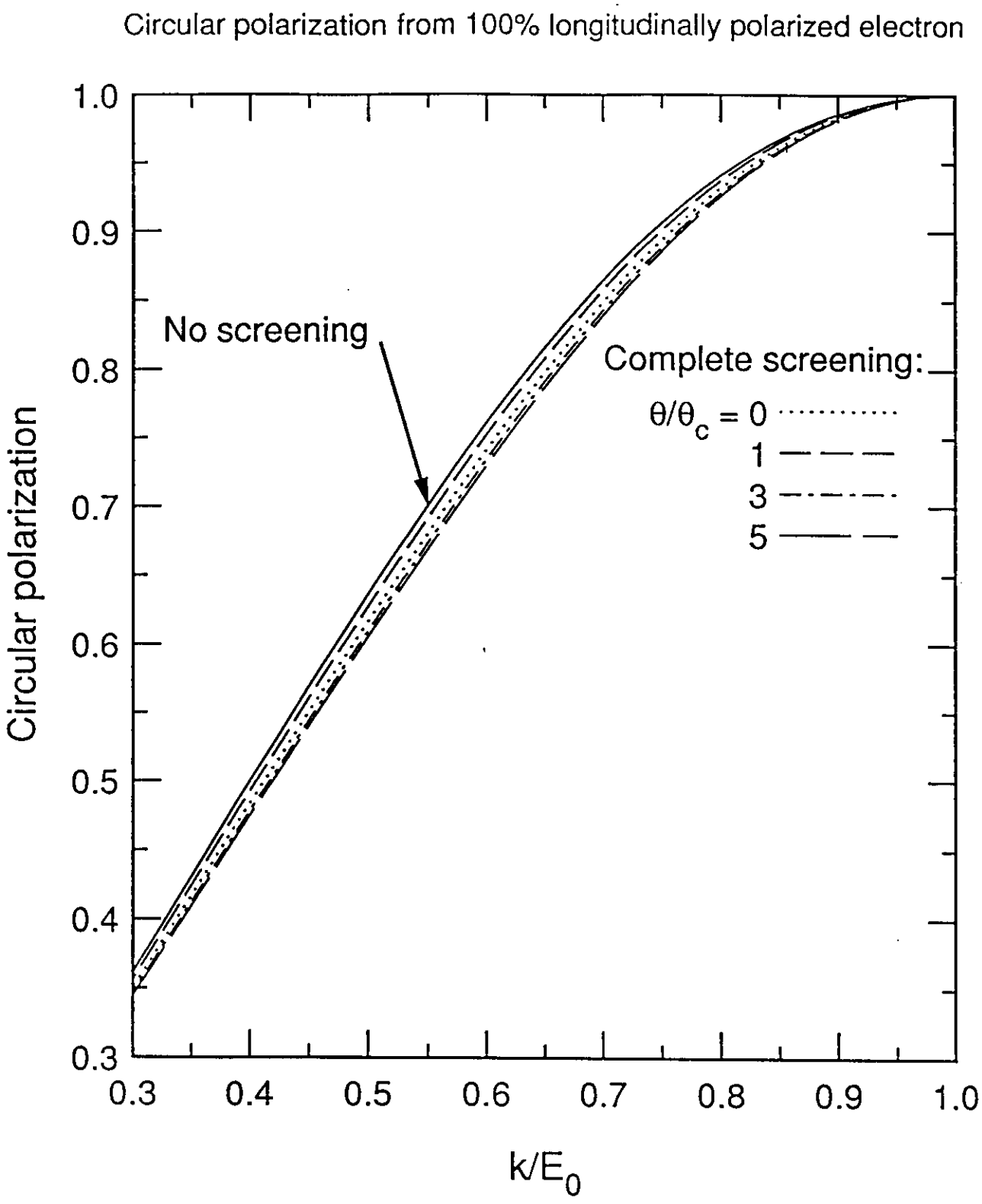

Figure 8. Circular polarization of bremsstrahlung from a 100% longitudinally polarized electron. The different "complete screening" curves (calculated from the formulas of Olsen and Maximon[17]) show the dependence on photon emission angle in units of $\theta_c = m_e/E_0$.

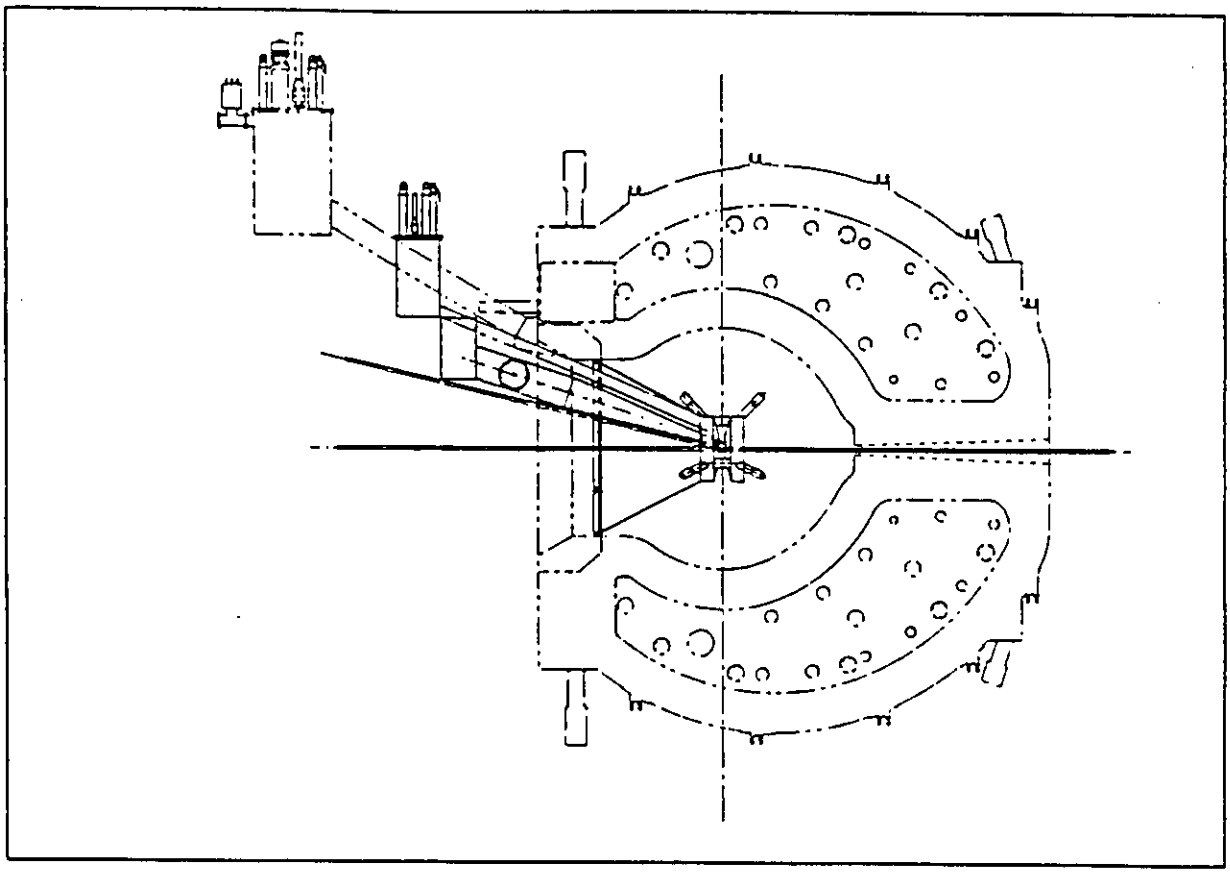

Figure 9. Proposed arrangement of high-field polarized proton target (target cryostat, superconducting magnet, support structure) inside the CLAS. The proposed experiment could use this system, but would be improved by using a low-field frozen spin target.

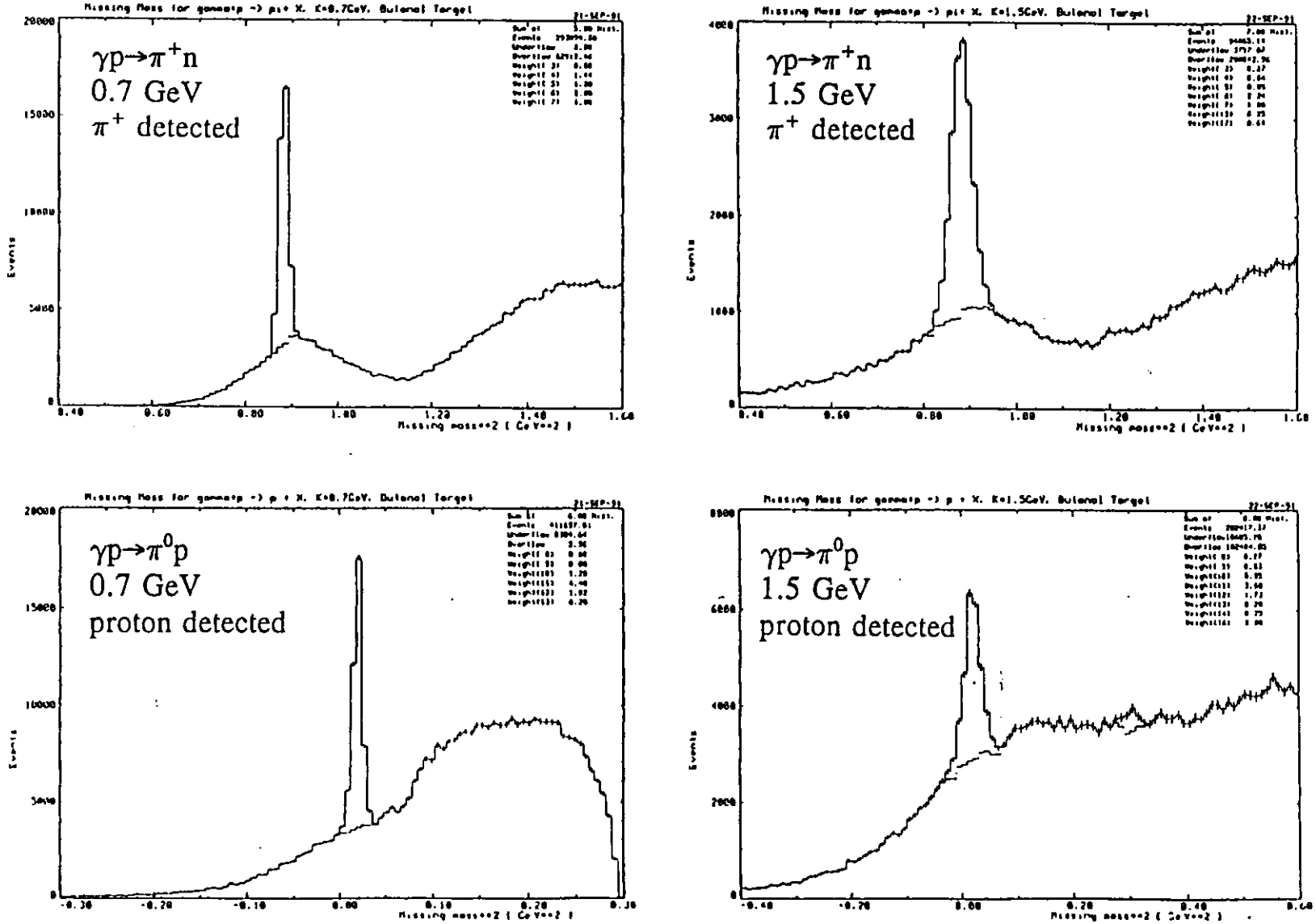

Figure 10. Monte Carlo simulations of missing-mass distributions used to separate the free-proton events from bound-nucleon background originating from a butanol target.